5. Godorr, S. A., Young, B. D. and Bryson, A. W., *Chem. Eng. Sci.*, 1990, **45**, 1793.
6. Meakin, P., *Phys. Rev.* 1984, **B30**, 4207.
7. Stanley, H. E. and Meakin, P., *Nature*, 1988, **335**, 405.
8. Borman, S., *Chem. Eng. News*, 1991, **69**, 28.
9. Pierce, P. E. and Schoff, C. K., *Euro Coat*, 1990, **3**, 101.
10. Laleq, M., Bricault, M. and Schreiber, H. P., *J. Coating Tech.*, 1989, **45**, 61.
11. Hammersley, J. M. and Handscomb, D. C., *Monte Carlo Methods*, Methuen, London, 1964.
12. Guell, O. A. and Holcombe, J. A., *Anal. Chem.*, 1990, **62**, 529A.
13. *Surface Coatings—Raw Materials and their Usage*, Oil and Colour Chemists' Association Australia, Chapman and Hall, London, 1974, vol. 1, p. 65.
14. Bauer, D. R. and Budde, G. F., *Ind. Eng. Chem. Prod. Res. Dev.*, 1981, **674**, 20.
15. Bauer, D. R. and Dickie, R. A., *J. Coating Tech.*, 1986, **41**, 58.
16. Mukesh, D., Srinivasan, K., Ghogare, A. and Gadkari, R. G., *J. Coatings Tech.*, 1991, (submitted).
17. Bauer, D. R., *Progr. Organic Coatings*, 1986, **193**, 14.
18. Bauer, D. R. and Dickie, R. A., *J. Polym. Sci.*, 1980, **18**, 1997.
19. Sagues, F. and Costa, J. M., *J Chem. Educ.*, 1989, **66**, 502.
20. Bird, R. B., Stewart, W. E. and Lightfoot, E. N., *Transport Phenomena*, Wiley International edn, New York, 1960.

ACKNOWLEDGEMENTS. We thank ICI India Limited for financial support and Mr A. Ghogare for preparing the films.

Received 18 March 1991; revised accepted 25 July 1991

Unusual growth of smectic A liquid crystals

R. Pratibha and N. V. Madhusudana

Raman Research Institute, Bangalore 560 080, India

Smectic A liquid crystals have been found to grow from the isotropic phase in the very unusual form of long *cylindrical structures in some* binary mixtures of smectogenic and non-mesomorphic aliphatic compounds. We report some experiments which show that the occurrence and stability of these structures can be accounted for by a concentration gradient of the non-mesomorphic component. In such a case it is necessary to include a *linear* term in curvature in the elastic energy density of the system.

SMECTIC A liquid crystals are characterized by a *layered* arrangement of long organic molecules which are approximately parallel to one another (Figure 1)[1-3]. The structure within the layers is that of a fluid, so that the medium is a 1D crystal (along the z-axis say) and a 2D liquid. In a perfect monodomain sample (Figure 1) the layers are flat and separated from their neighbours by a fixed spacing d, which is usually of the order of the molecular length. The elastic constant for compression along the layer normal is very large ($\sim 10^8$ erg cm^{-2}). On the other hand, the fluid layers can bend easily, preserving the layer spacing. The corresponding curvature elastic constant K is rather small ($\sim 10^{-6}$ dyne). Usually samples prepared between two glass plates have such bent layers, giving rise to point or line defects, about which the molecular orientation changes abruptly. The geometrical constraints require that the line defects form sets of confocal ellipses and hyperbolae[4].

When the smectic A phase separates from either the nematic phase which has only a long range orientational order, or the isotropic phase, it usually does so in the form of bâtonnets[4] (Figure 2) which are somewhat *elongated objects. This growth pattern has been studied* in great detail by Fournier and Durand[5] recently. The smectic A liquid crystal can be expected to have an anisotropic interfacial tension γ, and the formation of bâtonnets is a consequence of $\gamma_{\parallel} > \gamma_{\perp}$, where the subscripts $\parallel$ and $\perp$ refer to directions in relation to the layer-normal. The bâtonnets are structures in which the low value of K is exploited to minimize the area of the surface parallel to the layers exposed at the interface (Figure 3).

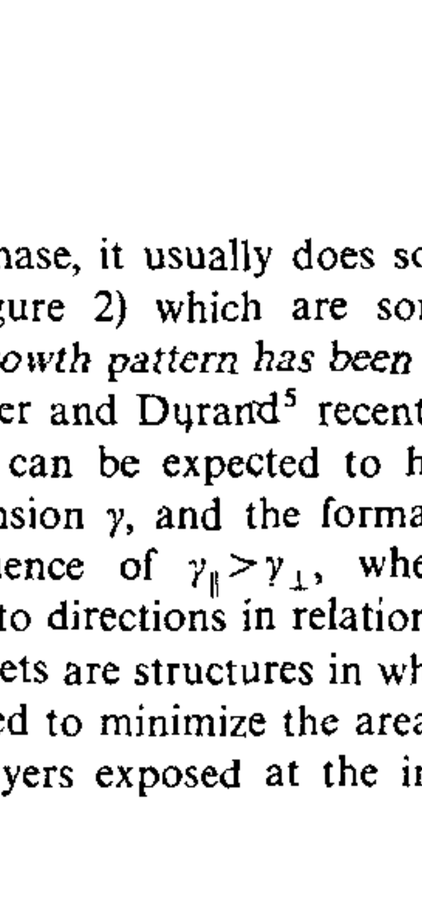

Figure 1. Schematic representation of the molecular organization in a smectic A liquid crystal

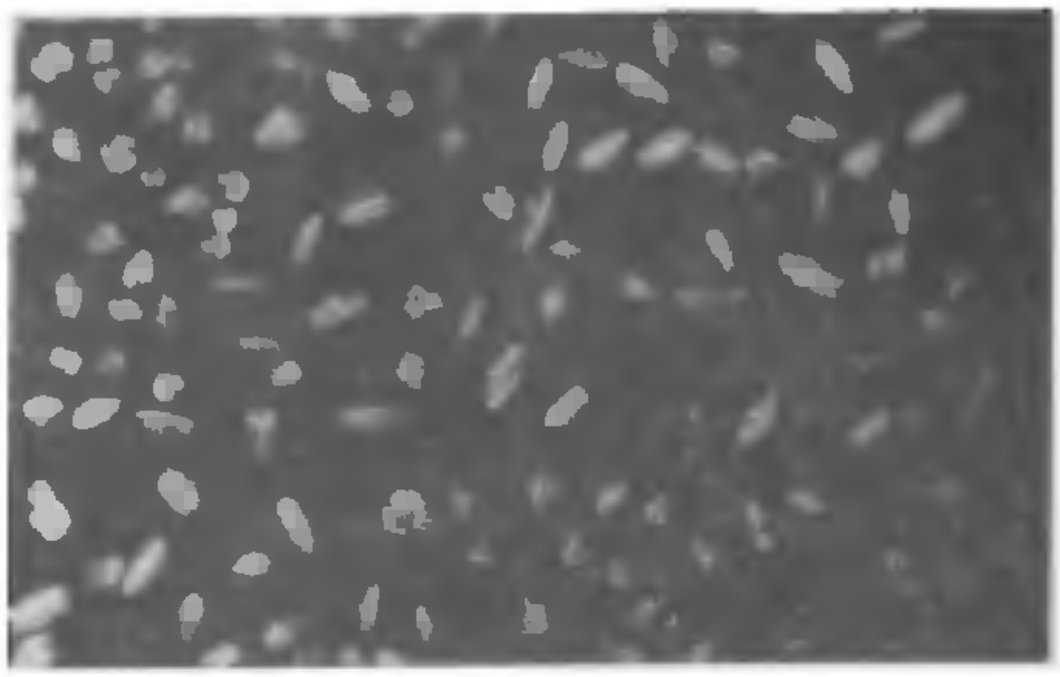

Figure 2. The smectic A phase separating out from the isotropic phase in the form of bâtonnets in a sample of diethyl azoxy dicinnamate (× 150).

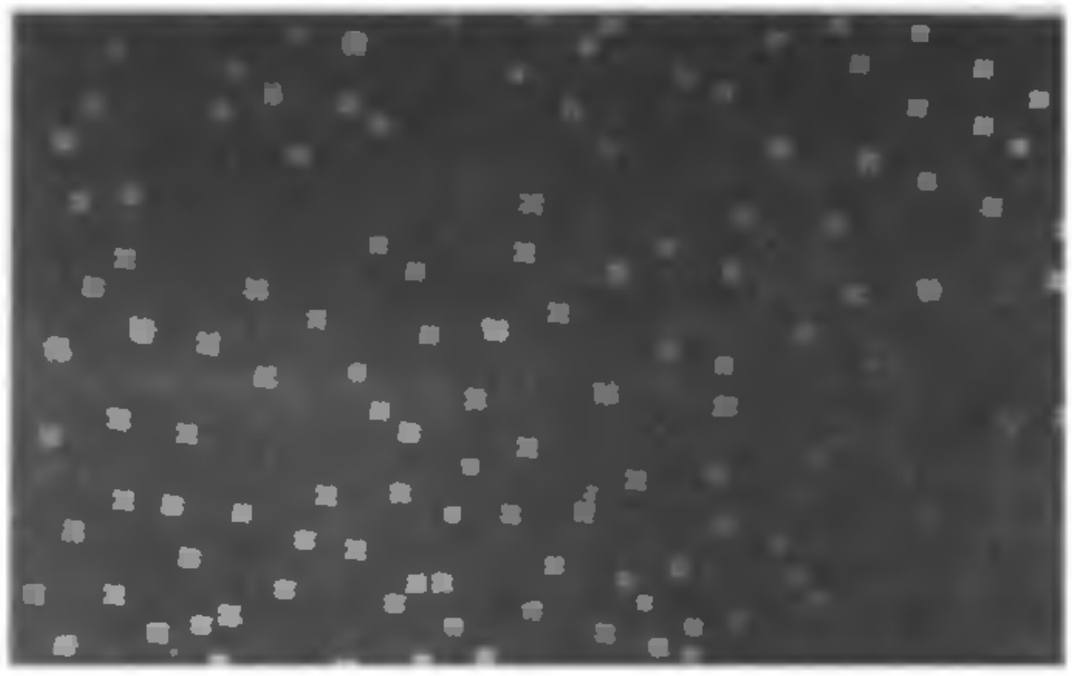

Figure 4. The smectic A phase appearing from the isotropic phase in the form of tiny spherical droplets in a mixture of 80CB and DODA in the molar ratio of 50.50. Crossed polarizers (× 150).

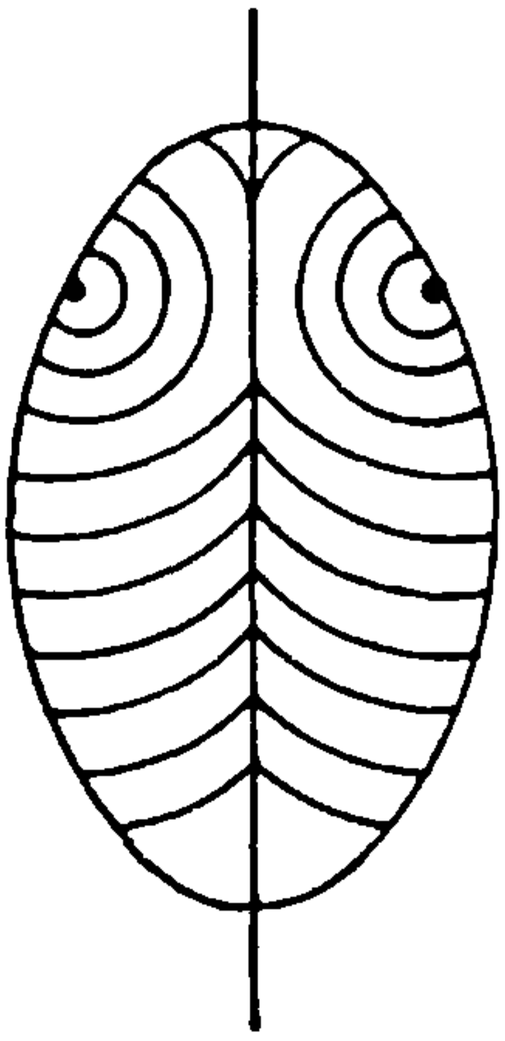

Figure 3. Schematic representation of the layers within a bâtonnet. (Adapted from Fournier and Durand, ref. 5).

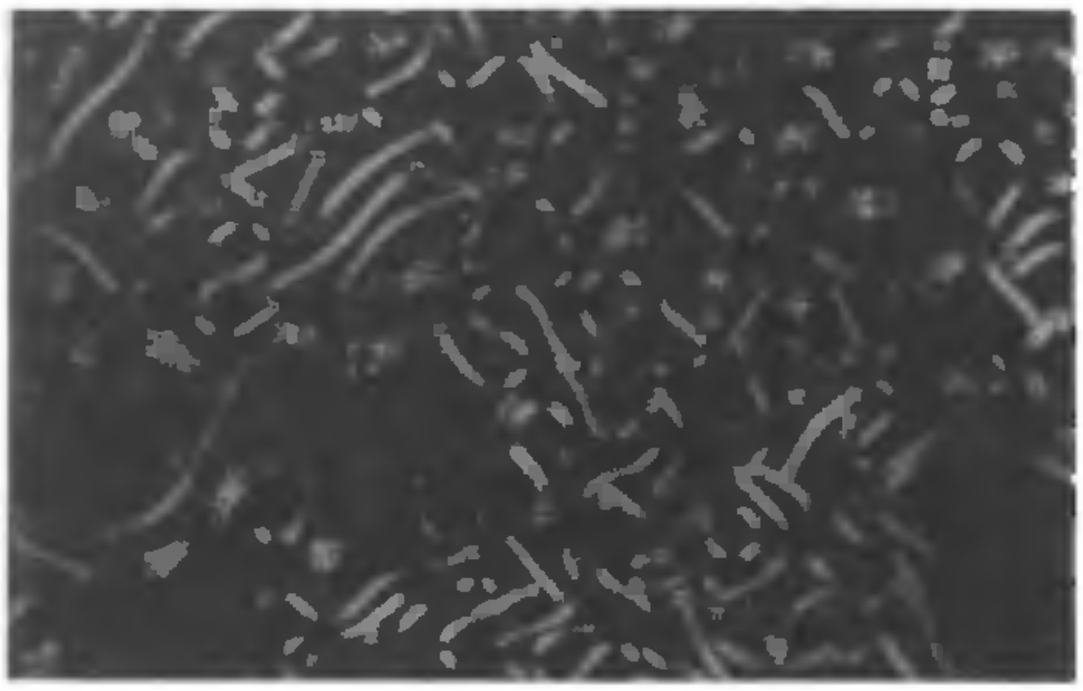

Figure 5. Rapid growth of the smectic A cylinders as the sample shown in Figure 4 is cooled.

We found some time back that binary mixtures of various smectogens with compounds having aliphatic chains (like alkyl alcohols, alkanes, alkanoic acids, etc.) exhibit a different growth pattern when separating from the isotropic phase when the concentration of the non-mesomorphic component is sufficiently large. The A phase separates first in the form of spherical droplets (Figure 4) which after attaining a certain diameter elongate to form cylindrical structures (Figure 5) as the sample is cooled at a fixed rate. The elongation takes place at a fixed diameter of the cylinder. A slow rate of cooling ($\sim 0.1^\circ\,\mathrm{min}^{-1}$) leads to very long structures ($\sim 500\,\mu$m or more) which collapse to form compact units. A higher rate of cooling ($\sim 1^\circ\,\mathrm{min}^{-1}$) leads to a large number of short cylinders which also collapse to form compact units. Indeed the first observation of such structures was made by Meyer and Jones in early 70s, but was reported only recently[6]. More recently Adamczyk[7] also reported similar observations. Arora *et al.*[8] found very shortlived cylindrical structures in a pure compound. Very recently such structures were also found in a pure compound synthesized in our laboratory[9].

We have made extensive observations on a 50 mole% mixture of dodecyl alcohol (DODA) with 4-*p*-octyloxy-cyanobiphenyl (80CB)[10]. The occurrence of the spherical and cylindrical structures with the surface parallel to the layers exposed to the interface clearly shows that in these systems $\gamma_{\parallel} < \gamma_{\perp}$, i.e., the sign of the anisotropy of interfacial tension changes at a high enough concentration of alcohol. We found that if the cooling is stopped at some temperature before the structure collapses, the further evolution of the cylinder depends on its diameter. Thin cylinders (with radius $r \leqslant 3\,\mu$m) shrink slowly and disappear over a period of

~ 30 min or so. On the other hand, thick cylinders (with $r > 4.5\ \mu m$) develop an undulation instability *about 10 min after the cooling is stopped (Figure 6)*. The structure then slowly collapses, bead by bead to a compact unit. If the cooling is resumed 10 min after it is stopped, even the thin cylinders develop a beaded configuration which collapses very quickly to form a compact unit. These observations seem to indicate that the cylindrical structures which have a large surface-to-volume ratio may be metastable with reference to the spherical units which minimize the surface area. Indeed, simultaneously with the occurrence of the above mentioned processes, flat homeotropic layers were found to grow from the two bounding glass plates. However, when we confined the liquid between glass plates which had corrugated surfaces (i.e., ground glass plates), the cylindrical structures could be stabilized for several hours at an appropriate temperature. Eventually, a focal conic texture developed at the glass surfaces at the expense of the cylindrical structures.

Figure 6. *a*, Smectic A cylinders formed in a mixture of 8OCB and DODA in the molar ratio of 50:50. *Photograph taken 10 min after* cooling was stopped. One thick cylinder has undergone the undulation instability. Polarizer axis is parallel to the horizontal edge of the photograph, no analyzer (× 60).

Figure 6. *b*, Same sample as in Figure 6*a* after another 5 s. The second cylinder has also undulated. Note that in the first structure, one of the beads has been absorbed into the big spherical unit. Polarizer axis perpendicular to horizontal edge of the photograph. No analyzer (× 60)

All these observations can be understood if we assume that the equilibrium alcohol concentration (x) in the smectic layers increases with the curvature of the layers, i.e., $x = x(r)$. This assumption implies that the cylindrical and spherical structures have a negative alcohol concentration gradient. We can turn around this argument to assume that a concentration gradient produces curvature in the layers. In other words, we have to add a term *linear* in curvature in the elastic energy density of such a system[10].

With the above assumption we get the following physical picture of the observations. As $\gamma_{\parallel} < \gamma_{\perp}$ in the mixtures, we can expect the smectic A to separate out in the form of spherical droplets from the bulk isotropic phase. The mixture with about 50 mole% of alcohol has a wide coexistence range of the smectic A and isotropic phases, the former having a lower temperature-dependent average concentration of alcohol than the latter. The spherical droplets grow by nucleating extra layers, which costs a nucleation energy. An alternative process of increasing the material in the smectic A phase at lower temperatures is to *absorb* additional molecules into the layers through the interface. If the number of layers is fixed, the spherical structure which has an isotropic core in the centre[4] can grow only by enlarging the core. As the alcohol concentration of the isotropic phase is higher and these molecules have to pass through the smectic layers from outside the sphere to the core, this mechanism cannot be very effective. However, if the structure can elongate along one direction to form a spherocylinder (Figure 7), the absorption process can become very efficient. Indeed it can be shown that the cylinder which has a line singularity along the axis requires less energy to grow than nucleating a new layer, if the radius is larger than a few microns[10]. Experimentally the radius is about 3 to 5 μm. Including the linear term mentioned earlier, the total energy of the cylinder is

$$E_{cyl} = 2\pi l\left[K_1(r - r_c) + \frac{K_{11}}{2}\ln\frac{r}{r_c} + \gamma(r + r_c)\right], \qquad (1)$$

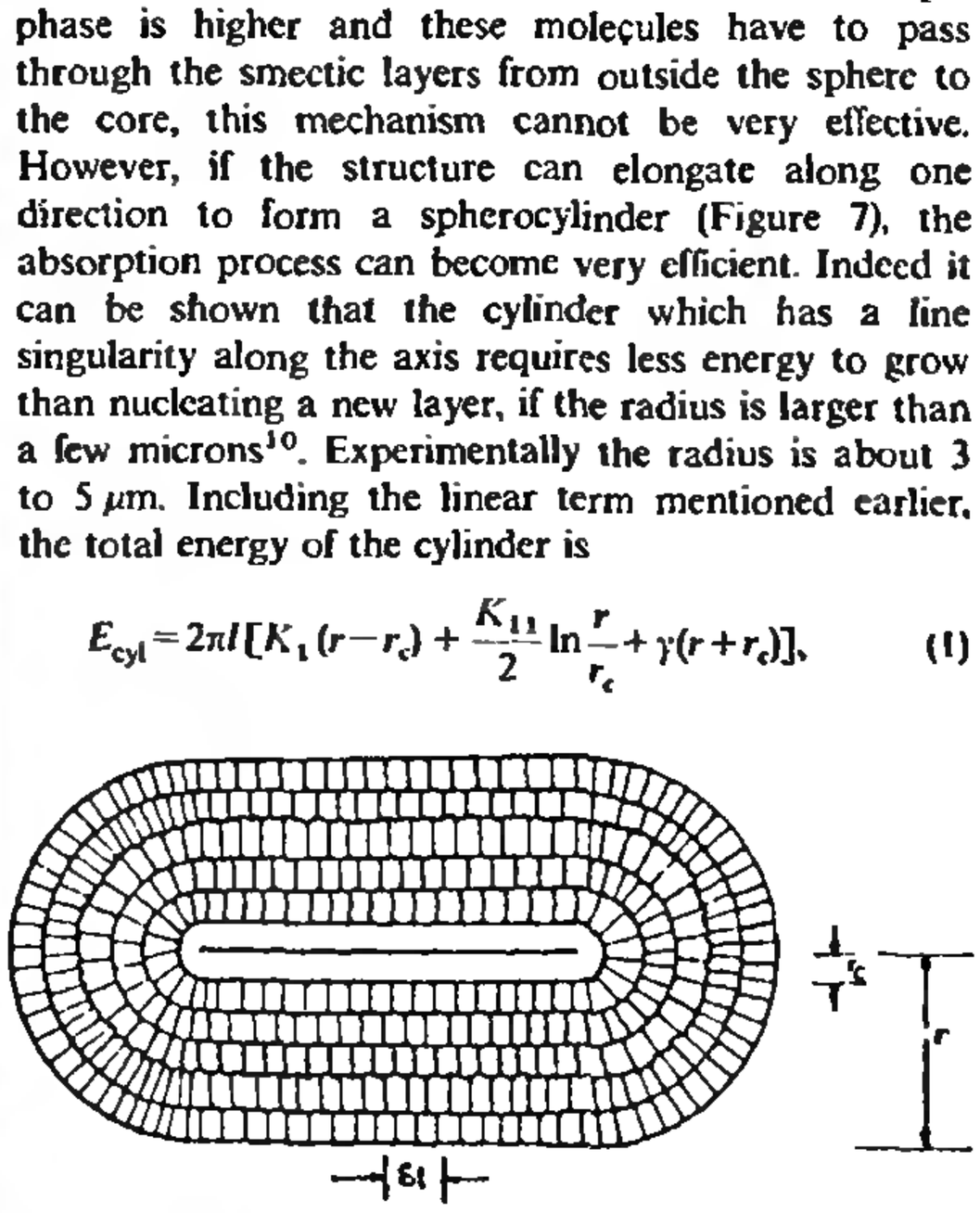

Figure 7. Schematic representation of a cross-section through the axis of the layer arrangement in a cylindrical structure.

where l is the length of cylindrical part, r and r_c are the radii of the cylinder and isotropic core respectively, K_1 the linear curvature elastic constant, K_{11} the (quadratic) curvature elastic constant and γ ($=\gamma$) the interfacial tension. If this cylinder collapses to form a spherical unit with a radius r_s and core radius r_{s_c}, the corresponding energy is given by

$$E_{sph} = 4\pi [K_1 (r_s^2 - r_{s_c}^2) + 2K_{11}(r_s - r_{s_c}) + \gamma (r_s^2 + r_{s_c}^2)]. \quad (2)$$

If $K_{11} \simeq 10^{-6}$ dyne[1], $\gamma \simeq 10^{-2}$ dyne cm^{-1} (ref. 11) and $l \simeq 100\,\mu$m, we find that the cylindrical structure has a *lower energy* than the spherical one if $K_1 < -0.02$ dyne cm^{-1}. This is a relatively small value which can easily be generated by the concentration gradient in the cylinders.

The growth of the cylinders requires that the absorbed mesogenic and alcohol molecules should reach the inner core from the outer surface through a diffusion process. The diffusion time τ ($\sim r^2/D$, where D is a diffusion constant) can be expected to be ~ 0.01 s for $r \simeq 3\,\mu$m. The elongation is indeed large for a slow rate of cooling ($\sim 0.1°$ min^{-1}). Faster rates produce many short cylinders.

Smooth glass plates apparently facilitate nucleation of flat layers. Since the alcohol concentration of such layers with zero curvature is relatively low, the growth of these layers increases the concentration of alcohol in the *isotropic phase* beyond the value required by thermodynamic equilibrium. This imbalance is corrected by dissolving cylinders and spheres of small radii. As the desorption of molecules from cylinders also requires a diffusion time τ, *thick* cylinders cannot dissolve at a fast enough rate. This results in a penetration of the alcohol molecules through the interface of the thicker cylinders to correct the imbalance mentioned above. This in turn results in a reversal of the concentration gradient, and hence the sign of K_1. As can be easily understood from Figure 8, such a sign reversal results in an undulation instability, since the regions with negative curvature have a higher average curvature than the regions with positive curvature. As the positive sign of K_1 cannot stabilize the cylindrical structure itself, it collapses to form a compact unit.

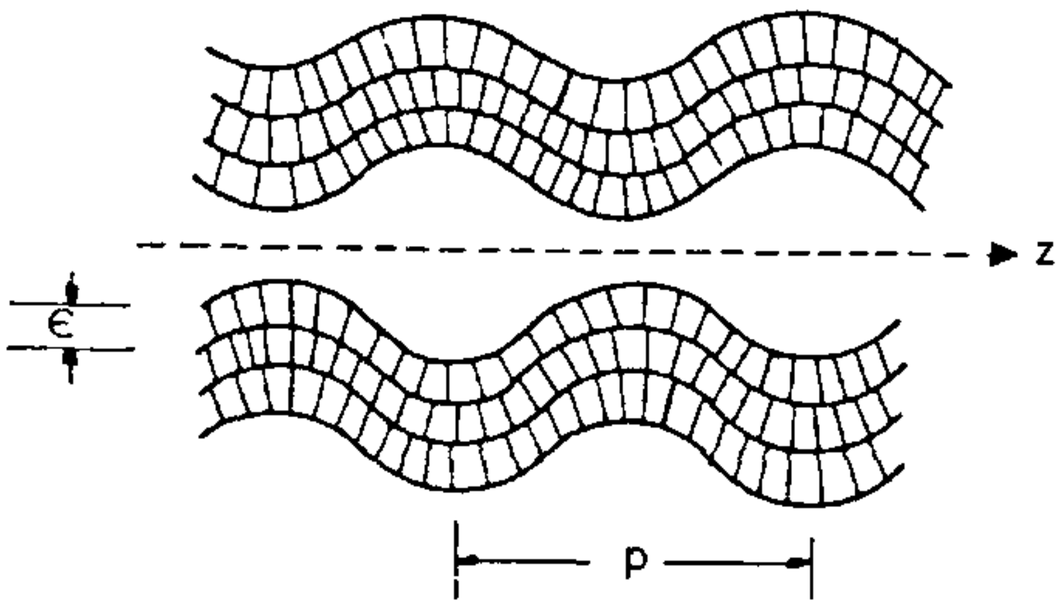

Figure 8. Schematic representation of the undulation instability of the layers in a smectic A cylinder.

In the samples taken between corrugated surfaces, the layers growing on the glass plates have a strong curvature and hence the alcohol concentration of the isotropic phase does not acquire the imbalance discussed above. The cylindrical structures remain stable for long periods in such a case. In order to test this model, we did some additional experiments recently on samples taken between two conducting glass plates. We measured the length of the cylinders at a fixed temperature as a function of time for various values of an applied AC voltage at 1 kHz. The results are shown in Figure 9. It is clear that the rate of shrinkage of the cylinder is faster at higher applied fields. The mesogenic compound used has a high positive dielectric anisotropy and hence would prefer to align with the long molecular axes along the field direction. However, the cylindrical structure itself cannot be altered as this would result in a change in layer spacing and hence require a prohibitively large energy. On the other hand, the field strongly favours the growth of flat layers on the glass plates. This in turn hastens the shrinkage of cylinders due to the process discussed earlier.

In conclusion, our experiments have shown that the equilibrium concentration of alcohol increases with curvature. We have argued that the resulting concentration gradient requires the inclusion of a term linear in curvature in the elastic energy density. For favourable values of this term, the cylindrical structures with a large surface/volume ratio are more stable than

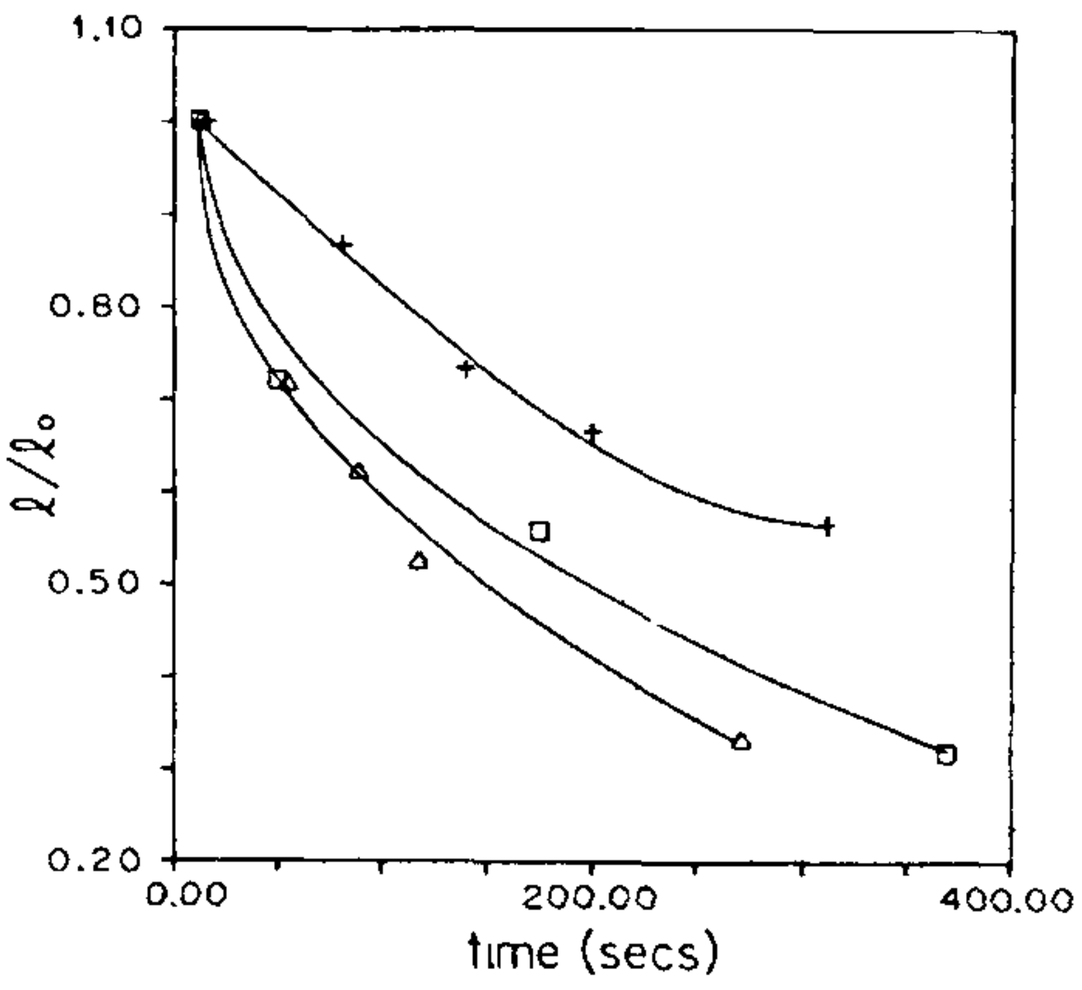

Figure 9. Plot of the ratio of l/l_0 vs. time for various values of an applied AC voltage at 1 kHz. Here l_0 is the initial length of the cylinder ($\sim 60\,\mu$m) and l is the length after time t. +, □ and △ correspond to $V = 0$, $V = 4$ and $V = 8$ volts respectively.

spherical structures even though the latter have the minimal surface area.

1. de Gennes, P. G., *The Physics of Liquid Crystals*, Clarendon Press, Oxford, 1975.
2. Chandrasekhar, S., *Liquid Crystals*, Cambridge University Press, Cambridge, 1977.
3. Friedel, G., *Ann. Phys.*, 1922, **18**, 273.
4. Kleman, M., *Points, Lines and Walls*, John Wiley, 1983.
5. Fournier, J. B. and Durand, G., *J. Phys.*, 1991, **1**, 845.
6. Meyer, R. B., Jones, F. and Palffy-Muhoray, P., Presented at the 13th International Liquid Crystal Conference, July 1990, Canada.
7. Adamczyk, A., *Mol. Cryst. Liq. Cryst.*, 1989, **170**, 53.
8. Arora, S. L., Palffy-Muhoray, P. and Vora, R. A., *Liq. Cryst.*, 1989, **5**, 133.
9. Veena Prasad and Sadashiva, B. K. (to be published).
10. Pratibha, R. and Madhusudana, N. V., *J. Phys.*, 1992, **2**, 383.
11. Faetti, S. and Palleschi, V., *J. Chem. Phys.*, 1984, **81**, 6254.

Received 3 March 1992; accepted 7 March 1992

Preparation of polypyrrole thin films by RF plasma polymerization

Ligy Cherian and P. Radhakrishnan

Department of Physics, Cochin University of Science and Technology, Cochin 682022, India

Doped polypyrrole is a conducting polymer. Polypyrrole films are usually prepared by electrochemical methods. *Here we report the deposition of polypyrrole thin films* on glass substrates using the RF plasma polymerization *method and its optical characterization. We also show* that the optical band gap of polypyrrole films decreases *from 2.8 eV to 0.8 eV as a result of iodine doping.*

CONDUCTING polymers are a class of materials, which while exhibiting characteristic features of polymers like light weight, great workability etc., also offer properties such as strength, elasticity, toughness, conductivity, etc. comparable to those of metals. Polypyrrole has a large band gap (3 eV). The band gap can be reduced by incorporating proper dopants like iodine. It has been reported that thin films of polypyrrole find applications in electro-optic devices[1]. These films have also been tested as coatings for gallium arsenide (GaAs) and silicon semiconductor electrodes.

Using the RF plasma polymerization method highly crosslinked, pinhole-free, ultrathin polymeric films have been prepared from a large number of organic and organometallic monomers[2]. This method is more economical due to the optimum use of monomer, high efficiency of polymerization and the absence of any type of catalyst. The experimental set-up used for film deposition (Figure 1) consisted of a deposition chamber made of borosilicate glass tube, a pumping system with associated pressure-measuring equipment, and an RF power supply designed to oscillate at 4.5 MHz with a maximum output of 35 W. The energy from RF power supply was capacitively coupled to the plasma by aluminium foils wrapped around the tube. The plasma current can be varied over the range 30–90 mA.

Clean, dry glass substrates were loaded in the deposition chamber and the system evacuated to a pressure of 5×10^{-2} torr up to the monomer container. The monomer vapour was then admitted into the chamber by opening the stopcock. When the pressure inside the chamber became steady (10^{-1} torr), the power source was switched on. Current and voltage were adjusted to get a fairly good uniform discharge. The monomer gets polymerized and deposits on the substrate. Freshly prepared polypyrrole films were doped with iodine by keeping the thin films in a glass chamber (20 cm length × 5 cm diameter) containing iodine vapour for about 10–15 min.

The absorption spectra of pyrrole monomer (Figure 2,*a*), polymerized pyrrole (Figure 2,*b*) and iodine-doped polypyrrole (Figure 2,*c*) were charted using a UV–VIS–NIR spectrophotometer (Hitachi 330 model) in the wavelength range 400–1200 nm. The spectrum of polypyrrole (Figure 2,*b*) is similar to that reported in literature[3]. The absence of the characteristic monomer bands in the polypyrrole spectrum shows that the monomer was polymerized. From this spectrum the band gap of the sample was determined to be approximately 2.8 eV. The observed increase in absorption for the doped sample was due to the incorporation of iodine into the polymer structure. The band gap of the doped sample determined using the spectrum was approximately 0.8 eV. In the present investigation, iodine-doped polypyrrole thin films were found to be stable to a great extent. The absorption spectrum and the approximate

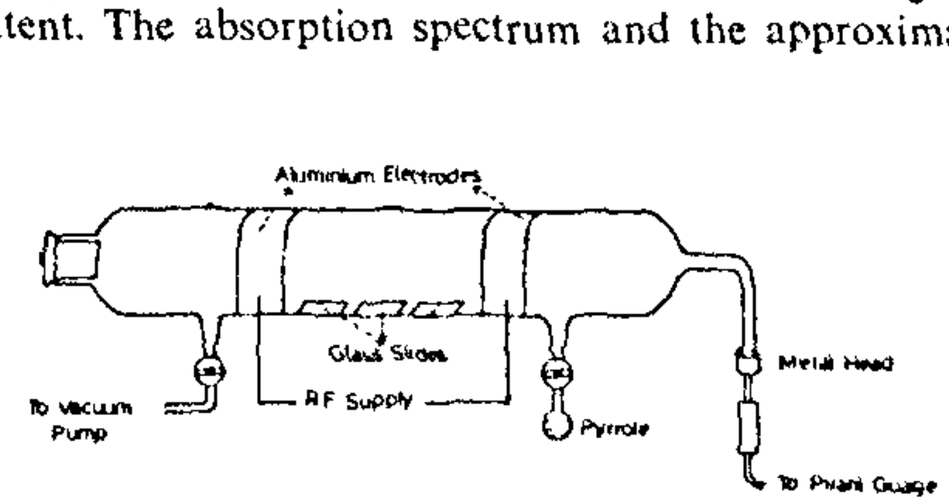

Figure 1. RF plasma polymerization set-up.